

Understanding the Behavior of Gas Sensors Using Explainable AI †

Sanghamitra Chakraborty *, Simon Mittermaier and Cecilia Carbonelli

Infineon Technologies AG, Munich, Germany

* Correspondence: sanghamitra.chakraborty@infineon.com

† Presented at the 9th International Electronic Conference on Sensors and Applications, 1–15 November 2022;

Available online: <https://ecsa-9.sciforum.net/>.

Abstract: Exposure to pollutants like ozone and nitrogen dioxide gas can cause serious health issues and harm the environment. Therefore, the interest in air quality and its impact on health and well-being has been steadily increasing over the years, making the low-cost gas sensing devices combined with artificial intelligence (AI) more and more popular due to their flexibility and small form factor. While AI provides state-of-the-art performance, it makes the system less transparent and more difficult to trust its decisions. With the aid of three different approaches, this paper seeks to understand and explain the predictions made by complex models for gas sensors. The use of such techniques can increase our confidence in the AI systems embedded in our products in terms of fairness or impartiality and robustness or reliability. This also improves our understanding of the sensor behavior and provide a more robust explanation for algorithm choices.

Keywords: Explainable AI; Interpretable AI; XAI; trustworthy AI; reliable AI; SHAP; Network Dissection; Bayesian Deep Learning; uncertainty quantification; gas sensors

Citation: Chakraborty, S.; Mittermaier, S.; Carbonelli, C. Understanding the Behavior of Gas Sensors Using Explainable AI. *2022*, *4*, x. <https://doi.org/10.3390/xxxxx>

Academic Editor: Francisco Falcone

Published date: 1 November 2022

Publisher's Note: MDPI stays neutral with regard to jurisdictional claims in published maps and institutional affiliations.



Copyright: © 2022 by the authors. Submitted for possible open access publication under the terms and conditions of the Creative Commons Attribution (CC BY) license (<https://creativecommons.org/licenses/by/4.0/>).

1. Introduction

The increasing quantity of air pollutants such as ozone (O₃) and nitrogen dioxide (NO₂) poses a serious threat to humans, animals, and plants in today's world, and therefore, it has become necessary to monitor these pollutant levels. Recently, low-cost gas sensors with graphene as the primary material have gained popularity to detect such pollutants, owing to their properties of good adsorption of gas molecules, low power consumption and low costs [1,2]. The graphene sensor under study consists of four sensing fields functionalized with different additional materials to trigger different chemical interactions between the sensor and the target gases. Gas molecules absorbed by the graphene sheet can have an influence on its electrical conductance, making it possible to use resistance as sensor signals. To avoid the potential saturation of graphene with gas molecules still on the surface, the sensor is heated to a high temperature periodically to accelerate desorption. Our application employs a recurrent neural network, namely a Gated Recurrent Unit (GRU) network [3], to estimate the concentrations of O₃ and NO₂ in parts per billion (ppb) using the features extracted from raw signals.

While artificial intelligence has gained significant traction over the years [4,5], the question of whether we can trust such sophisticated models owing to their lack of transparency persists. In recent years, many researchers have been developing novel methods to make models more interpretable and explainable [6–8]. Methods such as LIME (Local Interpretable Model-Agnostic Explanations) [9] have emerged to explain the predictions made by these models. Our paper uses three approaches to make our models reliable and trustworthy. These approaches helped us understand and improve the sensor behavior, and at the same time, develop more robust models.

The first approach is the Shapley Additive Explanations (SHAP) method, which ranks the features in order of their importance. This method was developed by Lundberg and Lee [10] and has been recently used in a variety of research, including finance [11] and healthcare [12]. The second method is to understand the internal architecture of our GRU network. This approach is highly inspired by the work of Karparthy et al. [13] on visualizing recurrent networks for text processing and Tang et al. [14] on memory visualization in speech recognition. The third approach aims to quantify the uncertainty of predictions made by our neural network, applying techniques from Bayesian Deep Learning [15]. Both Aleatoric and Epistemic Uncertainty are quantified and their meaning for the gas sensor is interpreted.

2. Methods and Results

2.1. SHAP Method

SHAP analysis estimates the individual contribution of each input feature to the overall prediction output using Shapley values [16]. The features are then ranked according to their contributions, with the highest estimates contributing more to model decisions and the lowest estimates either indicating that the features should be removed from the model or that more research is needed to raise their quality. The SHAP method is capable of calculating both local and global feature importance, where the former calculates the SHAP values of each of the data points and the latter determines for all data points and then averages the absolute values obtained [17]. We conducted our experiment to determine the global importance, and for this, fourteen features were extracted, namely, the relative resistances R0, R1, R2, and R3 for the four sensing fields, their corresponding first-order derivative, amplitude, phase and total harmonic distortion [18].

2.2. Results for SHAP Analysis

The feature ranking plot is shown in Figure 2 where the features are ordered in decreasing order of importance. Figure 2 shows R1 and its corresponding amplitude of first harmonic having the highest contributions, and R3 and its corresponding features having the least importance in the predictions, despite the fact that R3 is assumed to be a very significant feature since additional R3 characteristics like derivatives and frequency features are extracted from this core feature. Based on this analysis, the material of the fourth sensing field (R3) was improved, and as a result, it became one of the most stable fields in our sensor array. This can be seen in Figure 3, where the phase angle and relative resistance of this sensing field have the highest contributions to the predictions. Also, as seen in Figure 2, the SHAP analysis revealed that the features with higher-order (second and third) harmonics had little contribution to the predictions. This allowed us to remove these features, as shown in Figure 3, thereby allowing us to build a model that is both smaller and more efficient.

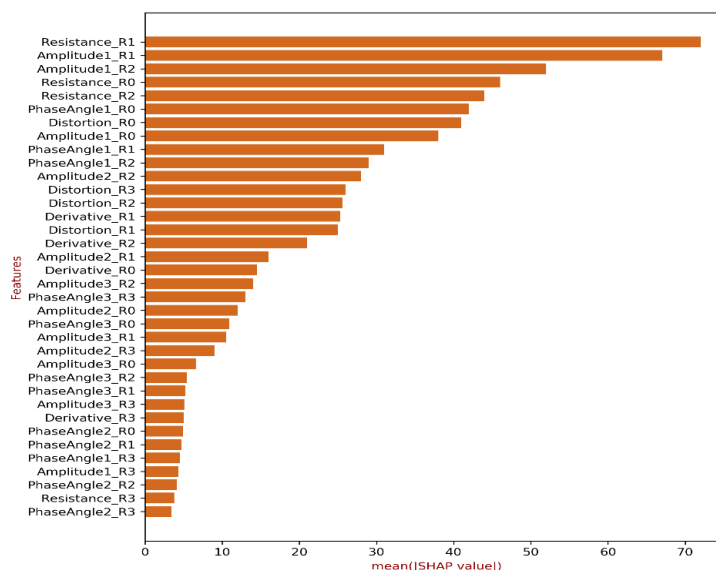


Figure 2. SHAP variable importance plot. The features include: Resistance, Derivative, Amplitude (n), PhaseAngle (n), and Distortion for each of the four sensing fields. Here, n = 1, 2, and 3, representing the 1st, 2nd, and 3rd harmonics.

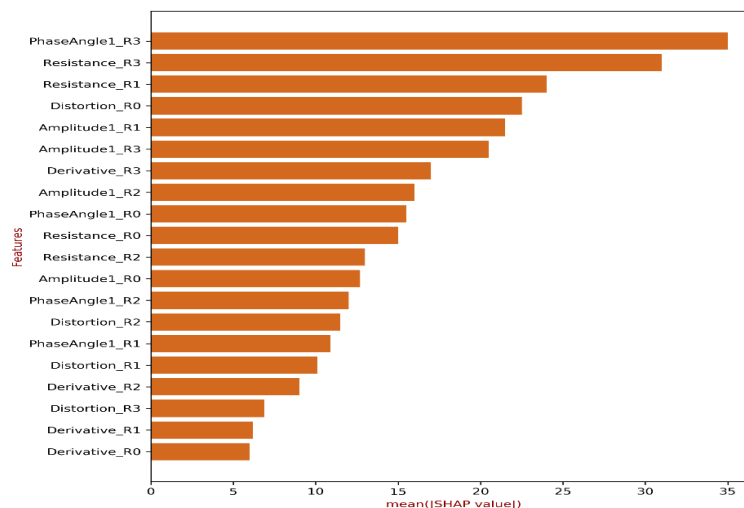


Figure 3. SHAP variable importance plot for model with reduced feature set and improved material.

2.3. Network Dissection

When using neural networks for predictions, we know the inputs and the outputs. However, we are not aware of what happens internally that makes such models reach specific decisions. This makes it challenging to understand why a certain prediction did not meet our expectations. Our research aimed to address this issue by inspecting the network’s inner-architecture. As we employed GRU for the predictions in our application, we investigated its internal structure by examining the hidden state output of each GRU unit. As each unit reacts differently to each of the gases and their concentration levels, the goal is to understand which units are in charge of predicting one gas in the absence of another, when both the gases are not present, or when there is a mixture of both in the air. It is like doing reverse engineering in the sense that we first view the output layer and then analyze the hidden layer(s) based on the outcome of the output layer. Due to the inclusion of the tanh function in each candidate hidden state, which causes the output of each hidden state to range from -1 (negative activation) to 1 (positive activation) [19], we

formed two clusters, placing all positive activations in one and all negative activations in the other.

2.4. Results for Network Dissection

As shown in Figure 5, when there is almost no NO_2 , the activations of Unit 9 are positive (orange points), otherwise negative (blue points), whereas Unit 5 gives positive activations when there is no O_3 . Unit 3 is responsible for identifying the scenario when both the gases are absent, in which case, the activations are positive, and in the presence of both the gases, the activations are negative. When either of the two gases is absent, Unit 6 gives positive activations, otherwise negative. Unit 8 shows the patterns when there is a mixture of both gases, where the activations are negative when O_3 is below 90 ppb, and positive for above. In Unit 4, for a combination of no O_3 and NO_2 approximately above 8 ppb, the activations are negative, but as O_3 increases, these become positive. No unit showed such a pattern when there is a gradual increase in NO_2 ; this confirms that as O_3 increases, NO_2 slowly gets overshadowed by the model. This investigation confirms the general observation that chemical sensors typically struggle to detect NO_2 when O_3 concentrations are higher. Also, not all the units gave a human-level understanding, as in the case of Units 7.

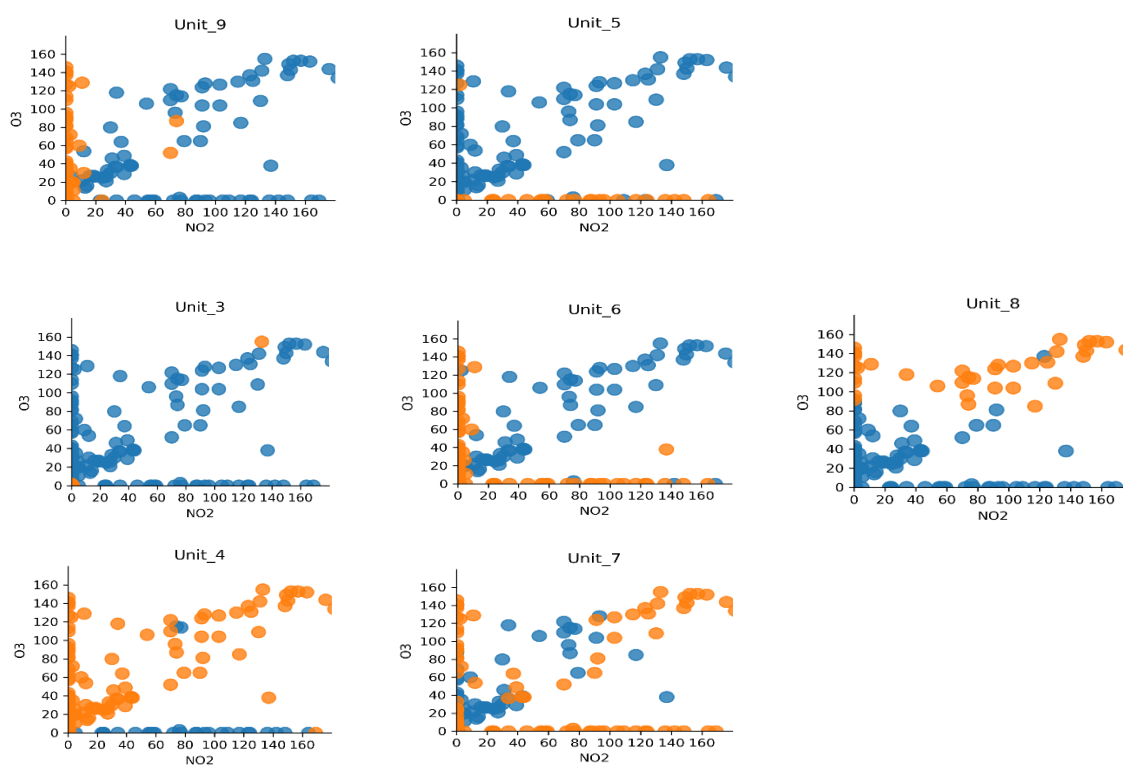


Figure 5. Activations of Units. The orange dots show positive activations and the blue dots show negative activations.

This analysis was also done with fewer units in the beginning, but it was difficult to make any interpretations because the patterns were not clearly distinguishable. This also sheds some light on hyperparameters optimization, like choosing the right number of units by understanding the network's behavior instead of simply using a heuristic approach.

2.5. Bayesian Deep Learning

Having now analyzed how input features impact model decisions via SHAP and visualized internal workings of the network via Network Dissection, techniques from

Bayesian Deep Learning can help us to provide a more interpretable and reliable output to our model by quantifying its uncertainty. Many applications require accurate but also reliable and trustworthy predictions. However, Machine Learning models are often over or under confident in their predictions and thus equipping models with the ability to tell a user when they are uncertain about their predictions leads to higher trust for the use of AI in safety critical environments. Bayesian Deep Learning provides such techniques for uncertainty quantification in neural networks [15].

Uncertainty can be divided into Aleatoric Uncertainty (Data Uncertainty), which refers to the data's inherent randomness that cannot be explained away. (e.g., noise) and Epistemic Uncertainty (Model Uncertainty), which refers to the uncertainty of the model and is affected by model choices and amount of training data.

Aleatoric Uncertainty in neural networks can be evaluated by designing the network to have an output neuron for mean and variance and training it with a log-likelihood loss function [15]. The Aleatoric Uncertainty information is represented in the corresponding variance.

Evaluating Epistemic Uncertainty is more challenging, as it requires modeling posterior distributions over weights. This becomes computationally intractable and therefore needs to be approximated. Gal & Ghahramani present an approximation method called Monte Carlo Dropout [20]. Dropout is known for being a regularization technique used during training, where random neurons in the network are ignored or "dropped" to avoid overfitting [21]. In contrast to its original intent Dropout can also be used during inference to drop random neurons each time the network is used for a prediction, resulting in a different network for each prediction. Using this to perform multiple predictions on the same data, we can statistically evaluate the variance between predictions and interpret this as the Epistemic Uncertainty.

2.6. Results for Bayesian Deep Learning

For the gas sensors under study, the Data Uncertainty is reflected in the different reaction of individual sensors to the same gas concentration, i.e., sensor-to-sensor variation and also in the same sensor reacting differently when exposed to the same gas concentration again, which can be due to previous saturation or aging. In contrast, by quantifying Model Uncertainty via Bayesian Deep Learning, we can identify specific situations in which our model performs poorly and plan tailored experiments to generate the right training data and improve the performance of the model in these situations, rather than blindly performing expensive and time-consuming measurements to generate more data overall. Figure 6 shows the model predictions for a given O₃ concentration profile. Both Aleatoric and Epistemic uncertainty are higher for higher concentrations, which means that the sensors response is less consistent for higher concentrations but also that more training data for higher concentrations would be beneficial for model performance.

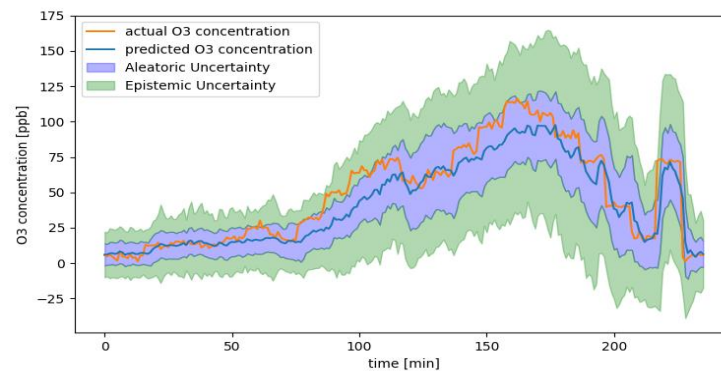


Figure 6. Model predictions (blue) for a given O₃ concentration profile (orange). Both the Aleatoric and Epistemic Uncertainty (light blue and green, respectively) are visualized by defining a region of $\pm 2\sigma$ of each uncertainty around the mean prediction.

3. Discussion

In this work, we presented three techniques that help with understanding why and how our model generates specific concentration predictions from a low-cost gas sensor.

First, we saw how SHAP analysis helps in the decision-making process of a model based on various input features and gives useful information on the underlying sensing mechanism and technology. Furthermore, the SHAP analysis aided in developing a more efficient model by identifying features that did not contribute much to the predictions, such as higher-order harmonics, and therefore, assisting in dropping off those features from the study. When working with smart sensors, such models with fewer dimensions are especially advantageous since they require less memory and processing power, thus, save energy.

The second approach helped dive inside the model's inner architecture. This method demonstrated that even black-box models like GRU can be quite transparent, making it still possible to trace the underlying rationale of its components.

Finally, we used approaches from Bayesian Deep Learning to quantify model and data uncertainty in our gas concentration predictions. This information allows to identify situations where more data is needed to improve the model via Epistemic Uncertainty as well as situations than cannot be improved with more data or different model decisions and therefore need to be solved on sensor technology level.

Author Contributions: Conceptualization, S.C., S.M. and C.C.; Methodology, S.C and S.M.; Software, S.C.; Validation, S.C., S.M. and C.C.; Formal Analysis, S.C and S.M.; Investigation, S.C and S.M.; Resources, C.C.; Data Curation, C.C.; Writing—Original Draft Preparation, S.C; Writing—Review & Editing, C.C. and S.M.; Visualization, S.C. and S.M.; Supervision, C.C. and S.M; Project Administration, C.C. All authors have read and agreed to the published version of the manuscript.

Funding: This research received no external funding.

Institutional Review Board Statement:

Informed Consent Statement:

Data Availability Statement:

Conflicts of Interest: The authors declare no conflict of interest.

References

1. Zöpfl, A.; Lemberger, M.M.; König, M.; Ruhl, G.; Matysik, F.M.; Hirsch, T. Reduced graphene oxide and graphene composite materials for improved gas sensing at low temperature. *Faraday Discuss.* **2014**, *173*, 403–414.

2. Hayasaka, T.; Lin, A.; Copa, V.C.; Lopez, L.P.; Loberternos, R.A.; Ballesteros, L.I.; Kubota, Y.; Liu, Y.; Salvador, A.A.; Lin, L. An electronic nose using a single graphene FET and machine learning for water, methanol, and ethanol. *Microsyst. Nanoeng.* **2020**, *6*, 50.
3. Cho, K.; Van Merriënboer, B.; Bahdanau, D.; Bengio, Y. On the properties of neural machine translation: Encoder-decoder approaches. *arXiv* **2014**, arXiv:1409.1259.
4. Jordan, M.I.; Mitchell, T.M. Machine learning: Trends, perspectives, and prospects. *Science* **2015**, *349*, 255–260.
5. Goodfellow, I.; Bengio, Y.; Courville, A. *Deep Learning*; MIT Press: 2016.
6. Murdoch, W.J.; Singh, C.; Kumbier, K.; Abbasi-Asl, R.; Yu, B. Definitions, methods, and applications in interpretable machine learning. *Proc. Natl. Acad. Sci. USA* **2019**, *116*, 22071–22080.
7. Doshi-Velez, F.; Kim, B. Towards a rigorous science of interpretable machine learning. *arXiv* **2017**, arXiv:1702.08608.
8. Lipton, Z.C. The myths of model interpretability: In machine learning, the concept of interpretability is both important and slippery. *Queue* **2018**, *16*, 31–57.
9. Malhi, A.; Kampik, T.; Pannu, H.; Madhikermi, M.; Främling, K. Explaining machine learning-based classifications of in-vivo gastral images. In Proceedings of the 2019 Digital Image Computing: Techniques and Applications (DICTA), Perth, WA, Australia, 2–4 December 2019; pp. 1–7.
10. Lundberg, S.M.; Lee, S.I. A unified approach to interpreting model predictions. In *Advances in Neural Information Processing Systems 30*; 2017.
11. Psychoula, I.; Gutmann, A.; Mainali, P.; Lee, S.H.; Dunphy, P.; Petitcolas, F. Explainable machine learning for fraud detection. *Computer* **2021**, *54*, 49–59.
12. Dave, D.; Naik, H.; Singhal, S.; Patel, P. Explainable ai meets healthcare: A study on heart disease dataset. *arXiv* **2020**, arXiv:2011.03195.
13. Karpathy, A.; Johnson, J.; Fei-Fei, L. Visualizing and understanding recurrent networks. *arXiv* **2015**, arXiv:1506.02078.
14. Tang, Z.; Shi, Y.; Wang, D.; Feng, Y.; Zhang, S. Memory visualization for gated recurrent neural networks in speech recognition. In Proceedings of the 2017 IEEE International Conference on Acoustics, Speech and Signal Processing (ICASSP), New Orleans, LA, USA, 5–9 March 2017; pp. 2736–2740.
15. Kendall, A.; Gal, Y. What uncertainties do we need in bayesian deep learning for computer vision? In *Advances in Neural Information Processing Systems 30*; 2017.
16. Shapley, L. 7. A Value for n-Person Games. Contributions to the Theory of Games II (1953) 307–317. In *Classics in Game Theory*; Princeton University Press: Princeton, NJ, USA, 2020; pp. 69–79.
17. Molnar, C. *Interpretable Machine Learning*; Lulu. com: 2020.
18. Vergara, A.; Martinelli, E.; Llobet, E.; D’Amico, A.; Di Natale, C. Optimized feature extraction for temperature-modulated gas sensors. *J. Sens.* **2009**, *2009*, 716316.
19. Tembhurne, J.V.; Diwan, T. Sentiment analysis in textual, visual and multimodal inputs using recurrent neural networks. *Multimed. Tools Appl.* **2021**, *80*, 6871–6910.
20. Gal, Y.; Ghahramani, Z. Dropout as a bayesian approximation: Representing model uncertainty in deep learning. In *International Conference on Machine Learning*; PMLR: 2016; pp. 1050–1059.
21. Srivastava, N.; Hinton, G.; Krizhevsky, A.; Sutskever, I.; Salakhutdinov, R. Dropout: A simple way to prevent neural networks from overfitting. *J. Mach. Learn. Res.* **2014**, *15*, 1929–1958.